ISSN: 2141 – 3290
www.wojast.com

APPLICATION OF MULTILAYER FEED-FORWARD NEURAL NETWORK TO PREDICT POROSITY AND WATER SATURATION VOLUMES IN PARTS OF ONSHORE NIGER DELTA.

EDET, O. E*., TAMUNOBERETON- ARI, I., AMAKIRI, A. R. C. AND AMONIEAH, J.
Department of Physics, Rivers State University, Port Harcourt, Nigeria.

*Correspondence: *thegreatmanofgod@gmail.com, +234 806 389 1823*

ABSTRACT

This study presents the successful implementation of a Multilayer Feed-Forward Neural Network to predict porosity and fluid saturation in two reservoirs using well log and 3D seismic data. By leveraging unknown nonlinear relationships in data between well logs and reservoir parameters, the technique accurately determines specific petrophysical features of reservoir rocks under various compaction conditions. Addressing the challenge of predicting petrophysical parameters, especially saturation, due to unclear correlations with seismic elastic characteristics, the research employed machine learning methods for seismic reservoir characterization. Prior to applying the neural network, seismic inversion was used to link geology, seismology, well-logs, and rock physics. The results identified hydrocarbon-bearing zones based on low acoustic impedance values. Training the neural network with six attributes for water saturation prediction and five for porosity prediction showed significant correlations, with actual and predicted water saturations and porosities having correlation coefficients of 72.6% and 80.6%, respectively. These parameters were then extended over reservoirs A and B to map their distribution in the field, proving the workflow's validity in accurately predicting water saturation and porosity.

KEYWORDS: Machine Learning, Niger Delta, Seismic inversion, Multilayer feed-forward network, Porosity.

INTRODUCTION

Reservoir characterization is building a reservoir model that incorporates all the characteristics of the reservoir that are pertinent to its ability to store and produce hydrocarbon. It is a difficult problem due to non-linear and heterogeneous subsurface properties and associated with a number of complex tasks such as data fusion, data mining, formulation of the knowledge base, and handling of the uncertainty (Chaki *et al*., 2014). The fundamental characteristics of a reservoir system are typically distributed spatially in a non-uniform and non-linear manner. Extraction of lithological information from available datasets is an important step in the reservoir characterization process. Since there is no direct measurement for the lithological parameters, they are to be computed from other geophysical logs or seismic attributes. This process also requires the development of algorithms to obtain the functional relationships between predictor seismic attributes and target lithological properties.

Machine Learning (ML) is defining a statistical or mathematical model based on data (Sarker, 2021). ML models are either trained in a supervised or unsupervised method. Supervised methods learn the functional mapping from x, being the data to y, being the ground truth or label for the data. When the ground truth is not known, unsupervised methods can be applied to determine structures and relationships within the data. Semi-supervised, and weakly supervised try to propagate partial labels to similarly distributed data and then learn the supervised mapping f(x) = y. Neural Network (NN) is a class of ML algorithms and are very diverse and versatile. Neural network analysis can significantly improve the seismic inversion result when the outputs of the inversion are used as external attributes in addition to regular seismic attributes for training the network (Mohamed *et al*, 2014, Mohamed *et al*, 2015, Mohamed *et al*, 2019). The neural network algorithm roughly mimics the way the human brain works, with its nonlinear, parallel processing approach. These networks are "trained" with data and a learning algorithm to work. It can predict other petrophysical parameters and it can be used for cross-validation process. Neural Networks (NNs) can be approached from several theoretical bases. Mathematically, NNs are directed acyclical graphs with edges and nodes. In neural computation, these are generally referred to as weights and nodes or neurons.

Neural Network (NN) learning algorithms have proved their validity and show significant accuracy in predicting various reservoir properties. The multilayer feed-forward neural network (MLFN) is one of them. As Hampson *et al*. (2001) mention that “the MLFN is the traditional network”. This type of network contains one or more of “hidden layers” between the input and output layers. Each layer consists of nodes (neurons), and the connection between the nodes of adjacent layers is set by weights. The procedure applied in this study involves three main steps which include finding the best set of attributes via multilinear regression technique, network training, and validation. This study applies the model-based inversion and a supervised neural network technique for porosity and water saturation (S_w) prediction from seismic data, to evaluate an already validated prospect in Niger Delta. A good understanding of the reservoir would further help improve upon the field reserved already recorded, at a reduced cost. The neural network methods proved its validity and accuracy through numerous published case studies (Hampson *et al*., 2001; Herrera *et al*., 2006; Dumitrescu and Lines, 2009; Mohamed *et al*., 2020, Akpan *et al*., 2022).

Location and Geology of the Study Area

The study area is located in the Offshore Niger Delta. The Niger Delta Basin is a tertiary delta located in the Gulf of Guinea and encompasses both the onshore and offshore areas of the Delta province, which is bounded by latitude 4° 0 to 7° 30 North and longitude 3° 0 to 9° 0 East. The Niger Delta is one of the world's hydrocarbon producing basins, dating back to the Tertiary period (Klett *et al*., 1997). It is located in Nigeria's southern region, which shares a border with the Atlantic Ocean (Figure 1a). The Niger delta is known to consist of three litho-units: an upper delta top lithofacies, an intermediate delta front facies and a deeper pro-delta lithofacies (Short and Stauble 1967; Reijers *et al*., 1996). Majority of the key hydrocarbon-bearing reservoirs in the delta exist within the Agbada Formation and are commonly situated in zones with structural heterogeneity. The formation consists mostly of channel and shoreface sands with slight shales in the upper part, and intercalation of shales and sands in equivalent ratio at the lower part of the basin Whiteman (1982). Structurally, the basin is subdivided into overlapping structural depo-belts that get younger and structurally complex southward (Figure 1b). The depo-belts are typically defined by syn-sedimentary growth faulting and folds that trend east–west direction. The development of the Delta, which has now resulted in a total thickness of more than 10 km, began during the Eocene. The upper Akata Formation, marine shales, and minor contributions from the interbedded marine shale beneath the Agbada Formation are the major source rocks in this region. The Agbada Formation sandstone facies is the primary oil target in the Niger Delta (Adiela and Odiri, 2018). However, turbidite sands of the upper Akata Formation are a potential target both offshore and likely deeper layers beneath the current Niger Delta producing onshore (Sunmonu *et al*, 2016). Figure 1c shows base map of wellbore distribution across the study area.

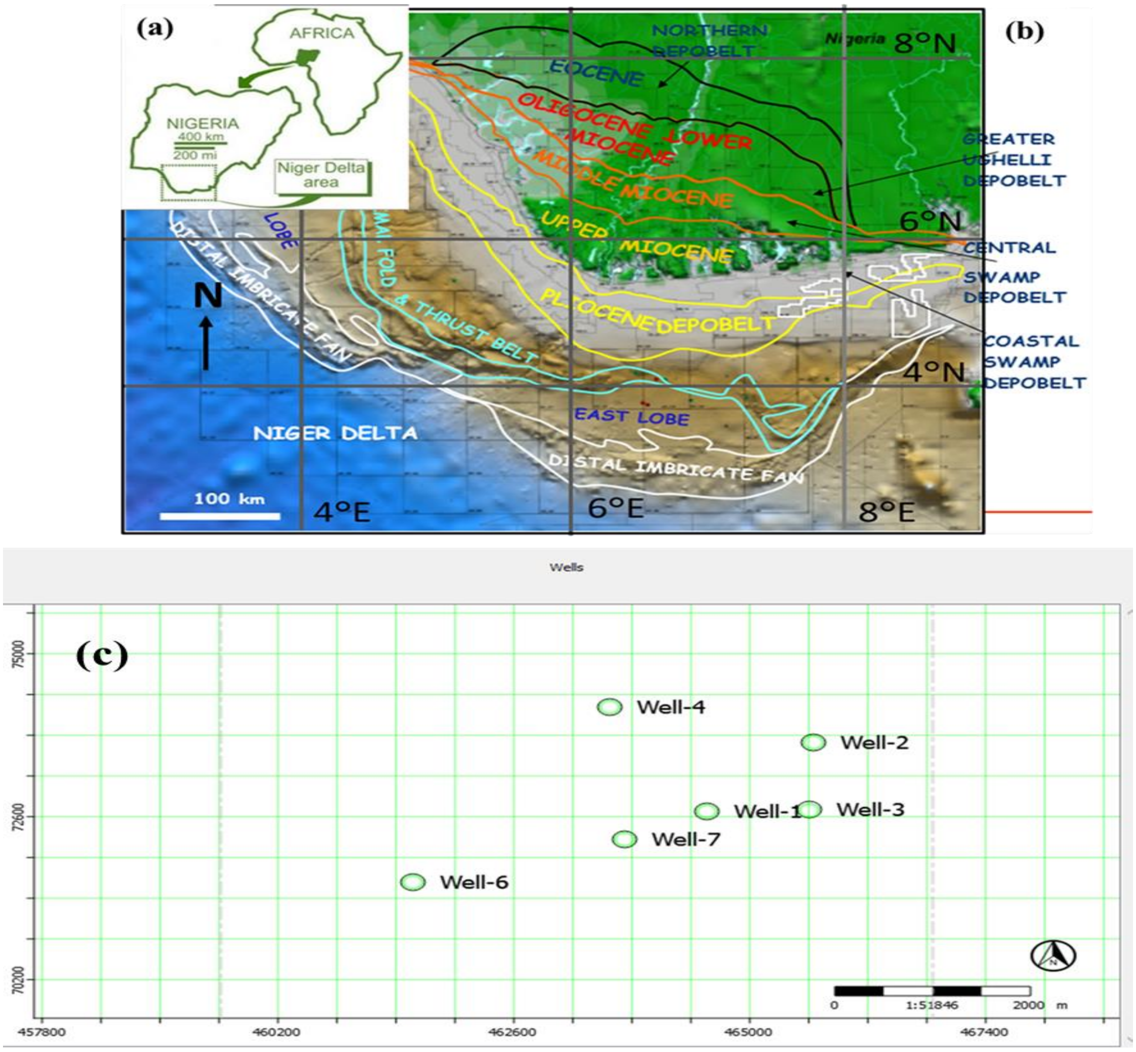

Figure 1: Location map of Niger Delta Basin (a) The inset shows Africa and Nigeria
(b) A Niger Delta Depobelt Map. (c) Base map showing wellbore distribution across the study area.

Theory of the Multilayer Feed-Forward Neural Network (MLFN)

In this study, the basic architecture of the MLFN also known as the traditional network was used that consists of three layers: the input, hidden, and output layers. The basic neural network architecture is illustrated in Figure 2, Each layer consists of nodes (neurons), and the connection between the nodes of adjacent layers is set by weights. The training process aims to find the optimum weights for those nodes (Hampson *et al*., 2001). The algorithm computes the weights for each layer that minimize the error between the output value and the training value. Mathematically, the input signals are multiplied by the synaptic (connection) weights; these weighted signals are then summed and have a nonlinear (activation) function applied to them as follows (Todorov, 2000):

$$y = f\left(\sum_{i=0}^{n-1} x_i w_i + w_n\right) \qquad (3)$$

where y is the neuron's output; x_i is the neuron inputs; w_i is the synaptic (connection) weights; i = ¼, 1… n − 1; w_n is a constant (bias); and f is an activation function. The weights are optimized by minimizing the prediction error. To avoid trapping in the local minima, MLFN uses a combination of simulated annealing and conjugate-gradient analysis to find the global minimum.

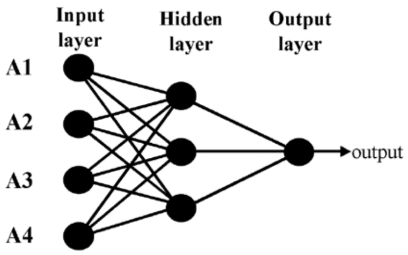

Figure 2**:** The basic neural network architecture (Todorov, 2000).

Materials and Methods

Data Sets

The study utilized six wells with total depths ranging from 11936.0 to 14950.5 MD ft and wireline petrophysical logs that penetrate the hydrocarbon reserviors of interest. These were the following logs available: Gamma-ray, density, compressional wave, resistivity, and caliper logs. The seismic-amplitude data made available to this study consist of full offset stack with a recorded duration of about 5200 milliseconds and sampled at 4ms. The inline and crossline numbers ranged between 4485 - 5524 and 1713 - 2033 respectively. Seismic inversion and neural network analysis rock physics analysis were performed using Hampson Russell Software (version 10.3.2). Hampson Russell Software is a powerful industry tool for rock physics and seismic inversion owned by CGG GeoSoftware.

Acoustic Impedance Inversion

Model-based inversion technique was used to derive acoustic impedance. The model-based inversion method is based on the convolutional model (Russell and Hampson, 1999). Model-based inversions use an iterative forward modelling and comparison procedure (Veeken and Da Silva, 2004). The procedure requires a starting model that is subsequently perturbed and checked against the seismic. This starting model is an interpolation of well data (probably with a low-pass filter applied). The final inversion result is a solution in which the impedance model has been checked against the seismic traces and the errors calculated and minimized. Pre inversion analysis was performed by running inversion at the well locations to QC and optimize the inversion parameters. The pre inversion analysis revealed a correlation of 98.8%. The display in Figure 3 shows the inversion result (in red) overlaying the original impedance log from the well from left to right. On the right, the selected wavelet (in blue), the synthetic traces generated from this inversion result (in red), and the original seismic composite trace (in black) are presented. Finally, the error trace is displayed, representing the difference between the two prior outcomes. The error is practically zero, as expected, demonstrating that the inversion is mathematically correct, i.e., this inversion produces a synthetic trace that matches the real trace.

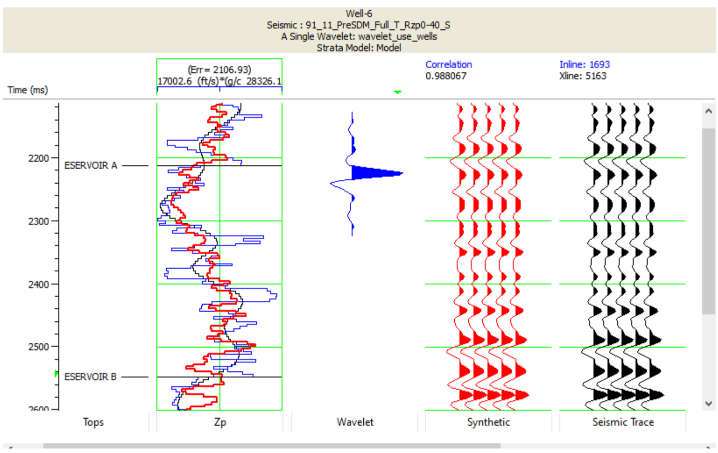

Figure 3: Pre-inversion analysis at well 6 from 2100-2600ms time interval

Neural Network Analysis

In this study, multilayer feed-forward neural network (MLFN) was applied to derive water saturation and porosity volumes. The input data include the well-log data, seismic full-stack, and acoustic impedance inverted volumes. MLFN contains one or more of "hidden layers" between the input and output layers (Hampson *et al.,* 2001). Each layer consists of nodes (neurons), and the connection between the nodes of adjacent layers is set by weights. The procedure applied in this study involves three main steps which include finding the best set of attributes via multilinear regression technique, network training, and validation. First, the most effective set of attributes were determined, which would predict the water saturation and porosity with the lowest prediction error. The attributes list includes internal attributes that are derived from the seismic full-stack data and external attributes. The technique used here is called multilinear regression. Accordingly, the provided ordering and number of attributes was used to train the neural network. Next, neural network algorithm was tested. After the training, there is the validation step, in which one-third of the well data were removed from the training step and then predicted blindly. This allowed us to find the number of statistically valid attributes. In the last step, the weights from the trained neural network were applied to the 3D seismic and inversion volumes. Figure 4 is a flowchart showing a summary of NN steps.

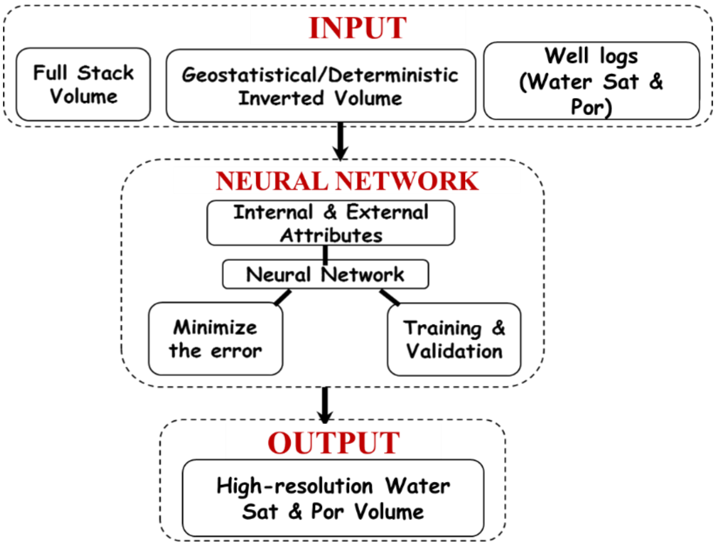

Figure 4: Flowchart showing a summary of neural network steps (modified from Mohamed *et al*., 2020).

RESULTS AND DISCUSSION

Acoustic impedance Inversion Cross-Section and Horizon Slice

The seismic inversion generates separate P-impedances of the survey with low frequency update from well log P-impedance initial models using the model-based inversion algorithm. A comparison is shown between seismic cross-section and inverted acoustic impedance section in Figure 5 and 6 resectively. The two inset wells are Well 3 and Well 6. As seen in figure 6, the zones in red, blue and purple are in increasing order of acoustic impedances, while zones in green to yellow have low impedance values. There is a variation in acoustic impedance from 19.2 to 27.1 × 10^3 (ft/s*g/cc). It is bounded by faults which act as structural traps for hydrocarbon. Acoustic impedance generally has high sensitivity to lithology and has the potential to fairly discriminate brine sands from hydrocarbon-charged sands. The acoustic impedance has elevated values, which ranged from 26.1 to 27.2 ×10^3 ft/s * g/cc with purple and blue colours corresponding to shales dominated formations. The intermediate values of acoustic impedance ranged between 22.1 and 24.1×10^3 ft/s * g/cc with red corresponding to shaley sands. The lowest acoustic impedance values are associated with hydrocarbon saturated sands, which have green and yellow colors in the range of 19.2 and 20.5 ×10^3 ft/s*g/cc. The log in the inverted section is the gamma ray log. The region around Well 3 has predominately shale compared to Well 6 which is made up of hydrocarbon sands with intercalation of shale. Figure 7 shows P-impedance attribute slice at the shallow reservoir (horizon A) while Figure 8 shows P-impedance attribute slice at the deep reservoir (horizon B). It is very clear that there is less hydrocarbon as depth increases, probably due to production. However, in both cases, there is the presence of low acoustic impedance around well 6 and well 7.

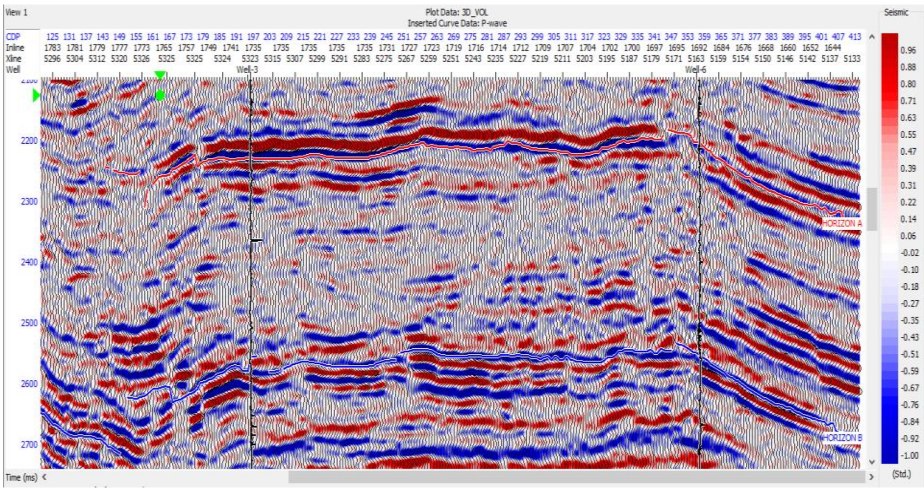

Figure 5: Seismic cross-section in variable density display, showing picked horizons (Horizon 1 and 2) as well as Well paths for wells 3 and 6.

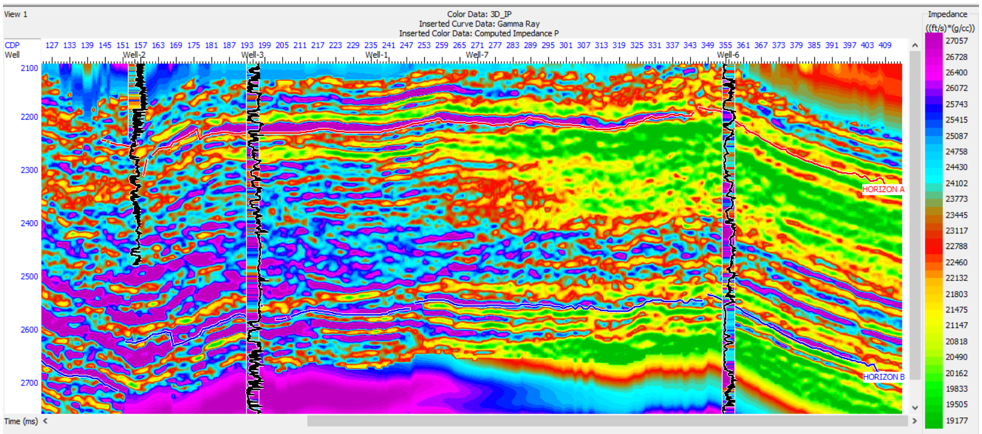

Figure 6: Acoustic impedance cross-section results with Gamma ray logs for well 3 and 6

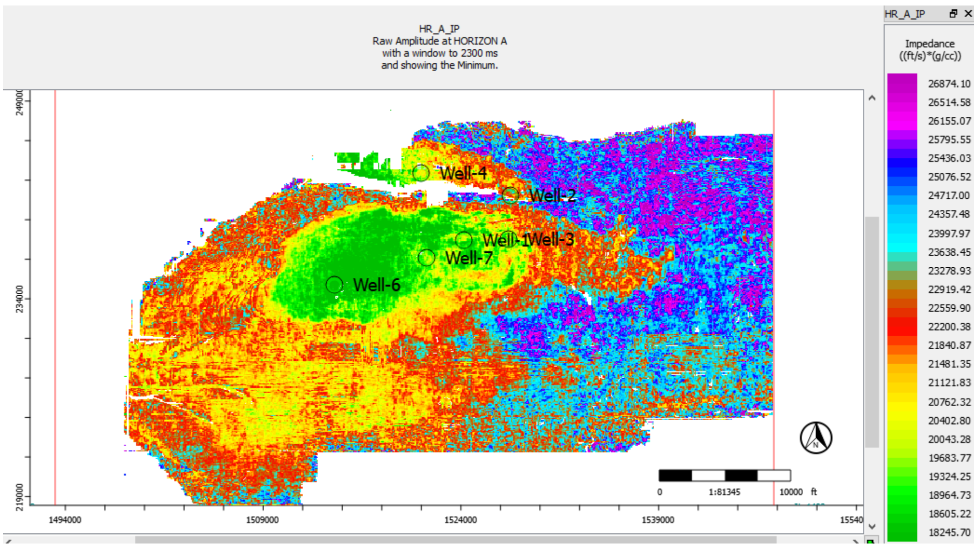

Figure 7: P-impedance attribute slice at the shallow reservoir (horizon A) with 5ms centred time window

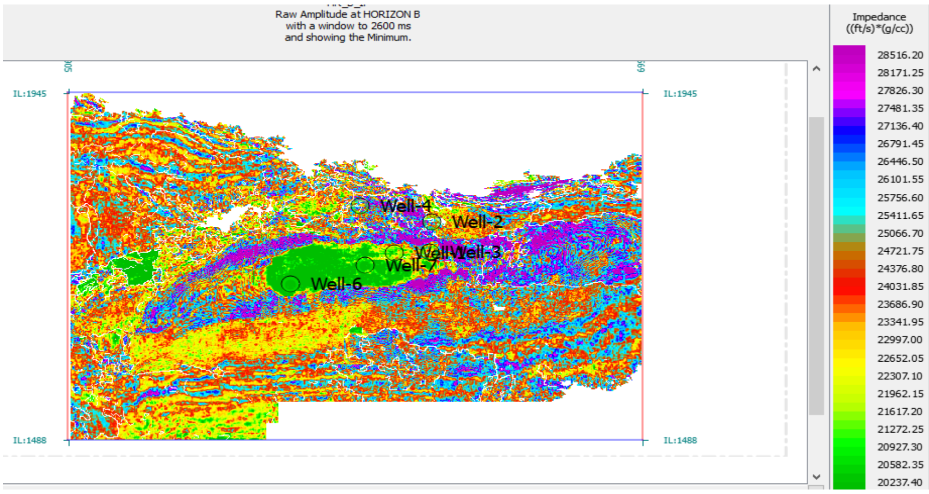

Figure 8: P-impedance attribute slice at the deep reservoir (horizon B) with 5ms centred time window

Multilayer feed-forward neural network (MLFN) Prediction

In this work, the MLFN's basic architecture was used, which comprises of three layers: input, hidden, and output. Each layer is made up of nodes (neurons), and the connection between nodes in adjacent levels is determined by weights. The training procedure seeks to determine the best weights for those nodes (Hampson *et al.*, 2001). The predicted porosity and water saturation from seismic, when cross-correlated with the well-derived porosity and water saturation, gave good correlations for MLFN each well. Figure 9 shows Original Water Saturation logs (x-axis) versus Predicted Water Saturation values (y-axis) for each well, showing 72.6% average correlation coefficient. Figure 10 shows original porosity logs (x-axis) versus Predicted porosity values (y-axis) with a correlation of 80.6%. The training of a neural network (NN) using six attributes in S_w prediction and using five attributes in porosity prediction showed a substantial number of correlations. The actual and predicted water saturations and porosities of the MLFN have correlation coefficients of 72.6 % and 80.6 %, respectively.

Water Saturation Prediction from MLFN

Figures 11, 12, and 13 show the outcome for water Saturation prediction from seismic using the MLFN algorithm. The cross-section line recovered from the produced porosity is depicted in Figure 11, overlaid with the reference wells 3 and 6 gamma ray logs placed along the well path. The horizon slice views of Horizon A and B are displayed in Figures 12 and 13, respectively. It is seen from the water saturation ranges from 0 to 100 %. The water saturation values vary around the cross-section with the eastern values having more lower values compared to the western regions. Within the prospective reservoir zone, water saturation values less than 40% were recorded, which is an indication of the possible presence of hydrocarbon especially around the well zones. Acoustic impedance is directly related to water status (Latimer *et al*. 2000). As a result, any increase in water saturation might be read as the partial or complete replacement of hydrocarbon with brine in reservoir pore spaces, resulting in an increase in acoustic impedance (Farfour *et al*., 2015). Within the well locations, the water saturation map retrieved from the generated volume (Figures 12 and 13 for shallow and deep reservoirs) indicates a value less than 20% (hydrocarbon saturation greater than 80%).

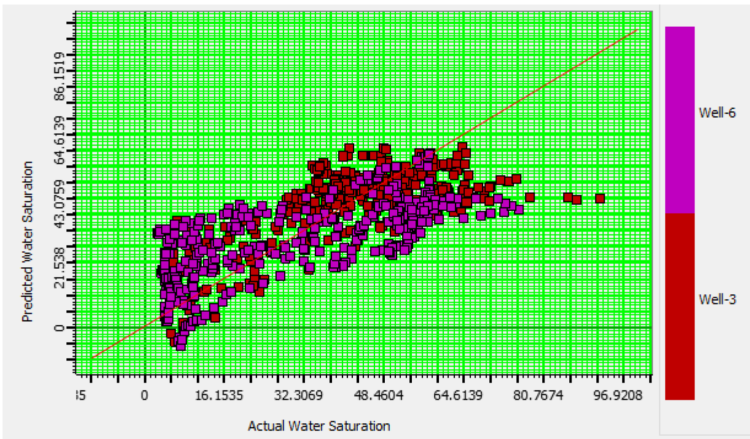

Figure 9: Original Water Saturation logs (x-axis) versus Predicted Water Saturation values

(y-axis) for each well, showing 72.6% average correlation coefficient.

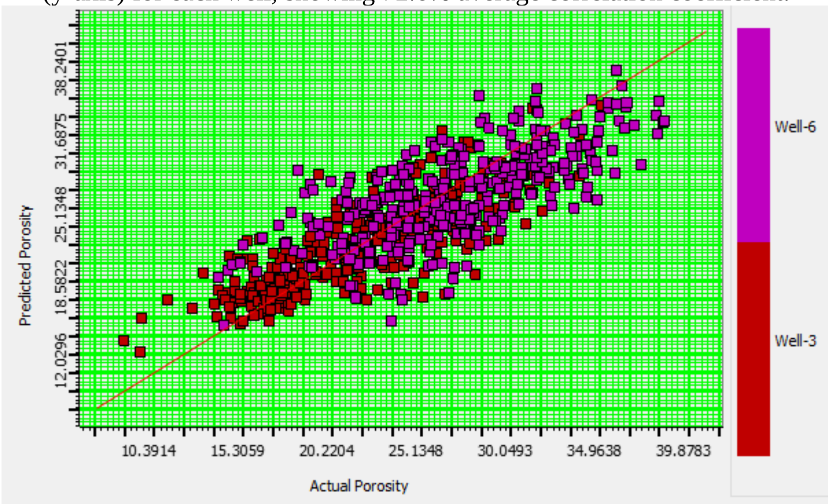

Figure 10: Original porosity logs (x-axis) versus Predicted porosity values (y-axis) with a correlation of 80.6%

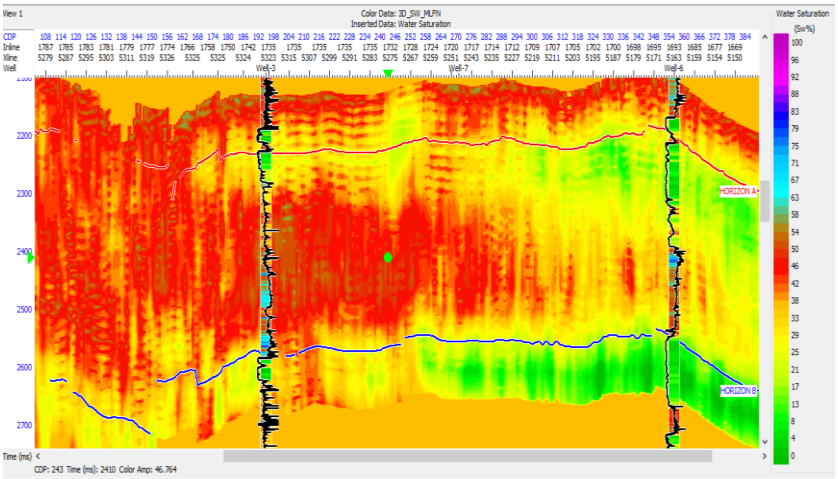

Figure 11: Water Saturation Predictions in cross-section view using MLFN

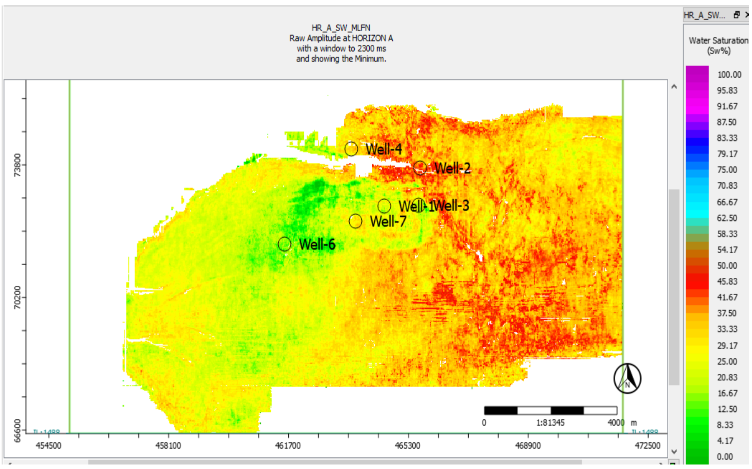

Figure 12: Water-saturation predictions in a map view using MLFN from Post Stack Inversion for Horizon A

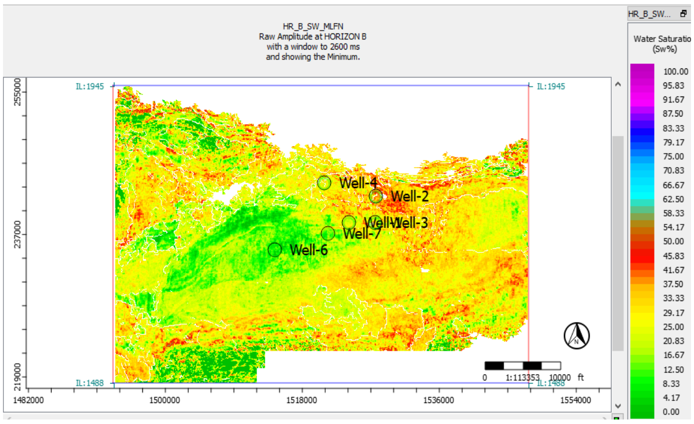

Figure 13: Water-saturation predictions in a map view using MLFN from Post Stack Inversion for Horizon B

3D Porosity Prediction from MLFN

The results of porosity prediction using the MLFN algorithm are illustrated in Figures 14, 15, and 16. Figure 14 displays a cross-section line from the generated porosity volume, with the porosity logs from reference wells 3 and 6 superimposed along their paths. Figures 15 and 16 provide horizon slice views of Horizons A and B, respectively. According to the color key, porosity ranges from 0 to 40%. The highest porosity values are observed around the drilled well in the exploited zone, indicating the presence of hydrocarbons and very low acoustic impedance (Ogbamikhumi *et al.*, 2018; Mavko et al., 2020). In the cross-section view, the porosity below Reservoir A is predominantly 35%, while around well 3, it ranges from 16 to 20%. This indicates that the region around well 6 is more porous compared to the area around well 3. The porosity in Horizon A ranges from 25% to 35%, while in Horizon B, it ranges from 16% to 25%. In both horizons, higher porosity values are concentrated on the eastern side of the field and around well 6.

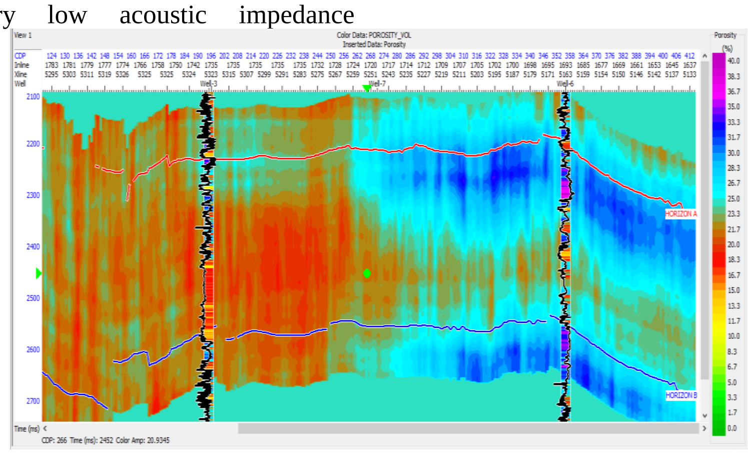

Figure 14: Porosity Predictions in cross-section view using MLFN

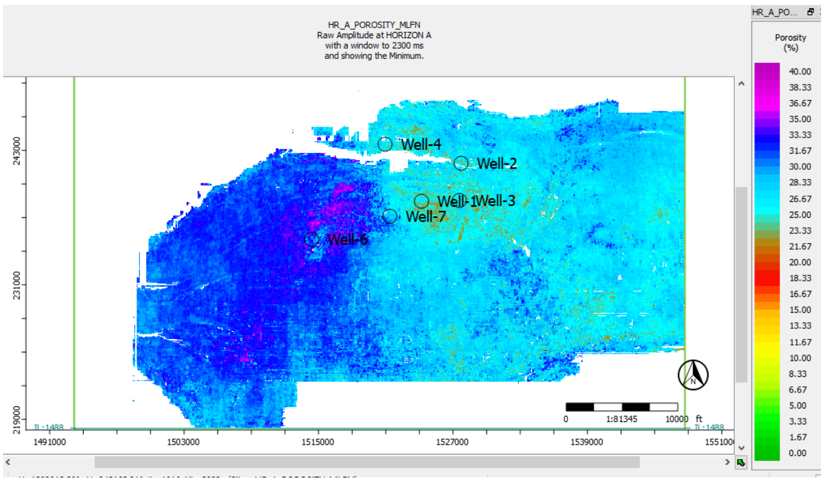

Figure 15: Porosity predictions in map view using MLFN from Post Stack Inversion for Horizon A

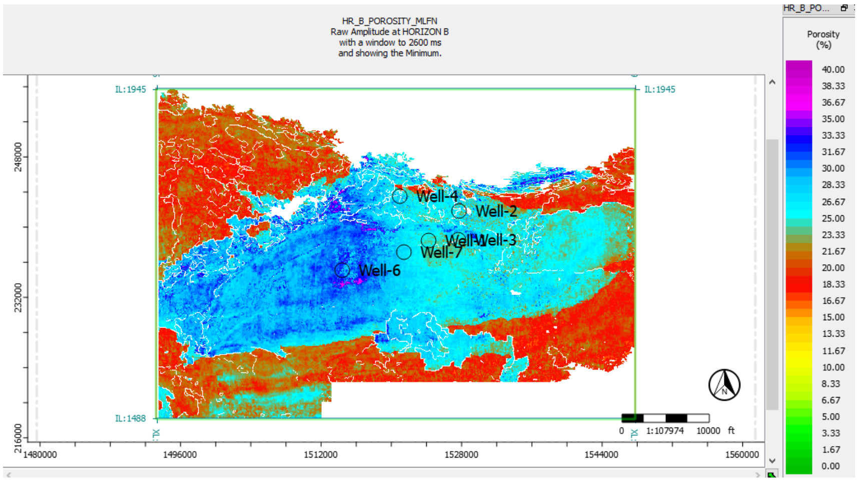

Figure 16: Water-saturation predictions in a map view using PNN from Post Stack Inversion for Horizon A

CONCLUSION

In this study, a novel scheme is proposed to improve the prediction of water saturation and porosity volumes using a machine learning algorithm. The novel scheme is called Multilayer Feed-Forward Neural Network and was used for the evaluation of an identified prospect in the undrilled area of the X field in the onshore Niger Delta Basin. Seismic inversion was utilized to derive acoustic impedance volume before neural networks were applied. Low values of acoustic impedance indicated hydrocarbon zones. A significant number of correlations were found when a neural network (NN) was trained using six attributes for S_w prediction and five attributes for porosity prediction. The correlation coefficients between the expected and actual water saturation and porosities of the MLFN are 82.6% and 72.6%, respectively. The distribution of these characteristics in X field was then described by extending the S_w and Porosity parameters over the reservoirs A and B. Hence, the integrated technique can be reliably adopted to predict reservoir properties to populate reservoir models for reserve estimation. Hence, it can be concluded that the prospective zone of the reservoir is marked with the presence of good quality hydrocarbon bearing reservoir.

ACKNOWLEDGMENTS

The authors acknowledge the support received from their colleagues in the Department of Physics at Rivers State University for their help with data interpretation, manuscript preparation, and editing. The authors are grateful to Shell Petroleum Development Company for granting permission to utilize the data used in this study. The author acknowledges *Hampson Russel* for the software used in this analysis.

REFERENCES

Adiela, U.P. and Odiri, N.A. (2018) Depositional environment and reservoir characterization of the Z10 Reservoir Sand, Niger Delta, Nigeria *International Journal of Pure and Applied Science and Technology*, 38 (10): 8-12.

Akpan, M. J., George, N. J., Ekanem, A. M. and Nathaniel, E. U. (2022). Utilizing Probabilistic Neural Network for Reservoir Assessment: A Case Study from an Onshore Niger Delta Field. *Researchers Journal of Science and Technology*, 2(3): 55–67. Retrieved from https://rejost.com.ng/index.php/home/article/view/41.

Chaki, S., Verma, A. K., Routray, A., Mohanty, W. K. and Jenamani, M. (2014). Well tops guided prediction of reservoir properties using modular neural network concept: A case study from western onshore, India," *Journal of Petroleum Science and Engineering*, 123: 155-163.

Dumitrescu, C. C., and Lines, L. (2009), Characterization of Heavy Oil Reservoir using V_p/V_s ratio and Neural Network Analysis: *CSPG-CSEG-CWLS Convention Abstracts*, 646–648.

Farfour, M., Yoon, W. J., & Kim, J. (2015). Seismic attributes and acoustic impedance inversion in interpretation of complex hydrocarbon reservoirs. Journal of Applied Geophysics, 114: 10.1016/j.jappgeo.2015.01.008.

Hampson, D. P., Schuelke, J. and Quirein, J. (2001). Use of multi-attribute transforms to predict log properties from seismic data: *Geophysics*, 66: 220–236, doi: 10.1190/1.1444899.

Herrera, V. M., Russell, B. and Flores, A. (2006). Neural networks in reservoir characterization: *The Leading Edge*, 25, 402–411, doi: 10.1190/1.2193208.

Klett, T.R., Ahlbrandt, T.S., Schmoker, J.W., and Dolton, J.L., 1997, Ranking of the world's oil and gas provinces by known petroleum volumes: U.S. Geological Survey Open-file Report-97-463.

Latimer, R., Davidson, R. and van Riel, P. (2000). An interpreter's guide to understanding and working with seismic-derived acoustic impedance. The Leading Edge, 19(3), 242-256. https://doi.org/10.1190/1.1438580

Mavko, G., Mukerji, T., & Dvorkin, J. (2020). The rock physics handbook. Cambridge University Press. https://doi.org/10.1017/9781108333016

Mohamed, I. A., El-Mowafy, H. and Fathy, M. (2015). Prediction of Elastic Properties using Seismic Prestack

Inversion and Neural Network Analysis. *Interpretation*, 3(2): 57–68. doi: 10.1190/INT-2014-0139.1.

Mohamed, I. A., El-Mowafy, H., Kamel, D. and Heikal, M. (2014). Prestack Seismic Inversion Versus Neural-Network Analysis: A Case Study in the Scarab Field Offshore Nile Delta, Egypt. *The Leading Edge*, 33: 498–506, doi: 10.1190/tle33050498.1.

Mohamed, I. A., Mahmoud, H., Ahmed, H. and Mohamed, R. (2019). High-Resolution Water-Saturation Prediction Using Geostatistical Inversion and Neural Network Methods. *Interpretation*, 7(2): 455–465.

Mohamed, I. A., Othman A, and Fathy M. (2020). A new approach to improve reservoir modeling via machine learning. *The Leading Edge*, 33: 170–175, doi.org/10.1190/tle39030170.1.

Ogbamikhumi, A., Andre-Obayanju, O., & Daniel, G. O. (2018). Fluid replacement modelling analysis for C4 reservoir characterisation onshore Niger Delta Basin. *Scientia Africana*, 17(2): 177-189.

Reijers T. J. A., Petter, S. W. and Nwajide C. S. (1996). The Niger Delta Basin. In T.J.A. Reijers (Eds.), Selected Chapters on Geology: Sedimentary Geology and Sequence Stratigraphy of Anambra basin (pp. 103-117). Warri, Nigeria: *SPDC Corporate Reprographic Services.*

Russell, B., & Hampson, D. (1999). Comparison of poststack seismic inversion methods. SEG Technical Program Expanded Abstracts, 10. https://doi.org/10.1190/1.1888870

Sarker, I.H. Machine Learning: Algorithms, Real-World Applications and Research Directions. *SN Computer Science*, 2: 160 (2021). https://doi.org/10.1007/s42979-021-00592-x

Short, K. C. and Stauble, A. J., (1967). Outline of Geology of Niger Delta: *American Association of Petroleum Geologists Bulletin*, 51: 761-779.

Sunmonu, L.A., Adabanija, M.A., Adagunodo, T.A. and Adeniji. A.A. (2016) Reservoir Characterization and by-passed pay analysis of Philus Field in Niger Delta, Nigeria. *International Journal of Advanced Geoscience*, 4 (2): 28-41.

Todorov, T. I., (2000). Integration of 3C-3D seismic data and well logs for rock property estimation: M.S. Thesis, *University of Calgary*.

Veeken, P. C. H. and Da Silva, M. (2004). Seismic inversion methods and some of their constraints. *First Break*, 22(6): 47–70.

Whiteman, A. (1982). Nigeria: Its Petroleum Geology, Resources, and Potential: London, Graham and Trotman, 394.